I R A M P
3(2), Dec. 2012, pp. 113-135

ISSN: 2229-3159

Effects of Plasma Screening on Circular States of Diatomic Rydberg Quasimolecules and their Application to Continuum Lowering in Plasmas

N. KRYUKOV AND E. OKS

Physics Department, 206 Allison Lab., Auburn University, Auburn, AL 36849, USA

ABSTRACT: In our previous works we studied analytically circular Rydberg states (CRS) of two-Coulomb-center systems consisting of two nuclei of charges Z and Z', separated by a distance R, and one electron. We obtained energy terms of these Rydberg quasimolecules for a field-free case, as well as under an electric field or under a magnetic field. The Rydberg quasimolecules of this type naturally occur in high density plasmas containing several types of ions, where a fully-stripped ion of the charge Z' is in the proximity of a hydrogenlike ion of the nuclear charge Z (or where a fully-stripped ion of the charge Z is in the proximity of a hydrogenlike ion of the nuclear charge Z'). Therefore in the present paper we study the effects of plasma screening on CRS of these Rydberg quasimolecules – the effects not taken into account in our previous works. We provide analytical results for weak screening, as well as numerical results for moderate and strong screening. First, the screening causes an additional energy term to appear – compared to the absence of the screening. This new term has a V-type crossing with the lowest energy term. Second, the internuclear potential is also affected by the screening, which destabilizes the nuclear motion for $Z > 1$ and stabilizes it for $Z = 1$. Third, we also study the effect of plasma screening on continuum lowering (CL) in the ionization channel. Calculations of CL evolved from ion sphere models to dicenter models of the plasma state. One of such theories – a percolation theory – calculated CL defined as an absolute value of energy at which an electron becomes bound to a macroscopic portion of plasma ions (a quasi-ionization). In 2001 one of us derived analytically the value of CL in the ionization channel, which was disregarded in the percolation theory: a quasimolecule, consisting of the two ion centers plus an electron, can get ionized in a true sense of this word before the electron would be shared by more than two ions [30]. It was also shown in [30] that, whether the electron is bound primarily by the smaller or by the larger out of two positive charges Z and Z', makes a dramatic qualitative and quantitative difference for this ionization channel. The results in [30] were obtained for circular states of the corresponding Rydberg quasimolecules. In the present paper we show that the screening decreases CL in the ionization channel, making CL vanish as the screening factor increases.

PACS numbers: 33.15.-e, 32.80.Ee, 52.25.-b, 32.60.+i

1. INTRODUCTION

Circular Rydberg States (CRS) of atomic and molecular systems, containing only one electron, have been extensively studied both theoretically and experimentally for several reasons (see, e.g., [1-18] and references therein). First, they have long radiative lifetimes and highly anisotropic collision cross sections, thereby enabling experiments on inhibited spontaneous emission and cold Rydberg gases. Second, these classical states correspond to quantal coherent states, i.e., objects of fundamental importance. Third, a classical description of these states is the primary term in the quantal method based on the $1/n$-expansion (n is the principal quantum number). Fourth, they can be used in developing atom chips.

In our previous works we studied analytically CRS of two-Coulomb-center systems, the systems (denoted as ZeZ') consisting of two nuclei of charges Z and Z', separated by a distance R, and one electron [2, 8, 11-13, 16, 17]. We obtained energy terms of these Rydberg quasimolecules for a field-free case, as well as under an electric field or under a magnetic field.

The Rydberg quasimolecules of this type naturally occur in high density plasmas containing several types of ions, where a fully-stripped ion of the charge Z' is in the proximity of a hydrogenlike ion of the nuclear charge Z

(or where a fully-stripped ion of the charge Z is in the proximity of a hydrogenlike ion of the nuclear charge Z'). Therefore in the present paper we study the effects of plasma screening on CRS of these Rydberg quasimolecules – the effects not taken into account in our previous works. We provide analytical results for weak screening, as well as numerical results for moderate and strong screening. We show that the screening leads to the following consequences.

The screening causes an additional energy term to appear – compared to the absence of the screening. This new term has a V-type crossing with the lowest energy term. The internuclear potential is also affected by the screening, which destabilizes the nuclear motion for $Z > 1$ and stabilizes it for $Z = 1$.

We also study the effect of plasma screening on continuum lowering (CL) in the ionization channel. CL was studied for over 50 years – see, e.g., books/reviews [19-23] and references therein. Calculations of CL evolved from ion sphere models to dicenter models of the plasma state [21, 24-29]. One of such theories - a percolation theory [21, 26] - calculated CL defined as an absolute value of energy at which an electron becomes bound to a macroscopic portion of plasma ions (a quasi-ionization). In 2001 one of us derived analytically the value of CL in the ionization channel which was disregarded in the percolation theory: a quasimolecule, consisting of the two ion centers plus an electron, can get ionized in a true sense of this word before the electron would be shared by more than two ions [30]. It was also shown in [30] that, whether the electron is bound primarily by the smaller or by the larger out of two positive charges Z and Z', makes a dramatic qualitative and quantitative difference for this ionization channel. The results in [30] were obtained for circular states of the corresponding Rydberg quasimolecules.

In the present paper we show that the screening decreases CL in the ionization channel, making CL vanish as the screening factor increases.

2. CALCULATION OF THE EFFECT OF PLASMA SCREENING AND CLASSICAL ENERGY TERMS FOR A RYDBERG QUASIMOLECULE IN A CIRCULAR STATE

Plasma screening of a test charge is a well-known phenomenon. For a hydrogen atom or a hydrogen-like ion (an H-atom, for short), it is effected by replacing the pure Coulomb potential by a screened Coulomb potential which contains a physical parameter – the screening length a. For example, the Debye-Hückel (or Debye) interaction of an electron with the electronic shielded field of an ion of charge Z is $U(R) = -(Ze^2/R)\exp(-R/a)$, where $a = (kT/(4\pi e^2 N_e))^{1/2} \approx 1.304 \times 10^4 (10^{10}/N_e)^{1/2} T^{1/2} a_0$, where N_e (cm^{-3}) and T (K) are the electron density and temperature, respectively.

We study a two-Coulomb center (TCC) system with the charge Z placed at the origin, and the Oz axis is directed at the charge Z', which is at $z = R$, the system being submerged in a plasma of a screening length a. We consider the circular orbits of the electron which are perpendicular to the internuclear axis and centered on the axis.

Two quantities, the energy E and the projection L of the angular momentum on the internuclear axis are conserved in this configuration. We use cylindrical coordinates to write the equations for both:

$$E = \frac{1}{2}(\dot{\rho}^2 + \rho^2\dot{\varphi}^2 + z^2) - \frac{Z}{r}e^{-r/a} - \frac{Z'}{r'}e^{-r'/a} \tag{1}$$

$$L = \rho^2\dot{\varphi} \tag{2}$$

where r and r' are distances from the electron to Z and Z'. The circular motion implies that $d\rho/dt = 0$; as the motion occurs in the plane perpendicular to the z-axis, $dz/dt = 0$. Further, expressing r and r' through ρ and z, and taking $d\varphi/dt$ from (2), we have:

$$E = \frac{L^2}{2\rho^2} - \frac{Z}{\sqrt{\rho^2 + z^2}}e^{-\sqrt{\rho^2+z^2}/a} - \frac{Z'}{\sqrt{\rho^2 + (R-z)^2}}e^{-\sqrt{\rho^2+(R-z)^2}/a} \tag{3}$$

With the scaled quantities

$$w=\frac{z}{R},\ p=\left(\frac{\rho}{R}\right)^2,\ b=\frac{Z'}{Z},\ \varepsilon=-\frac{ER}{Z},\ \ell=\frac{L}{\sqrt{ZR}},\ \lambda=\frac{R}{a},\ r=\frac{ZR}{L^2} \tag{4}$$

our energy equation takes the form below:

$$\varepsilon=\frac{e^{-\lambda\sqrt{w^2+p}}}{\sqrt{w^2+p}}+\frac{be^{-\lambda\sqrt{(1-w)^2+p}}}{\sqrt{(1-w)^2+p}}-\frac{\ell^2}{2p} \tag{5}$$

We can seek the equilibrium points by finding partial derivatives of ε by the scaled coordinates *w*, *p* and setting them equal to zero. This will give the following two equations.

$$\frac{we^{-\lambda\sqrt{w^2+p}}}{w^2+p}\left(\frac{1}{\sqrt{w^2+p}}+\lambda\right)=\frac{b(1-w)e^{-\lambda\sqrt{(1-w)^2+p}}}{(1-w)^2+p}\left(\frac{1}{\sqrt{(1-w)^2+p}}+\lambda\right) \tag{6}$$

$$\frac{\ell^2}{p^2}=\frac{e^{-\lambda\sqrt{w^2+p}}}{w^2+p}\left(\frac{1}{\sqrt{w^2+p}}+\lambda\right)+\frac{be^{-\lambda\sqrt{(1-w)^2+p}}}{(1-w)^2+p}\left(\frac{1}{\sqrt{(1-w)^2+p}}+\lambda\right) \tag{7}$$

From the definitions of the scaled quantities (4), we have $\ell^2 = 1/r$ and $E = -(Z/R)\,\varepsilon$. Since $r = ZR/L^2$, then $E = -(Z/L)^2\,\varepsilon/r$, where $r = 1/\ell^2$ can be obtained by solving (7) for ℓ. Thus, the scaled energy without explicit dependence on *R* is ε/r, which we shall denote ε_1. Using this, equations (5), (6) and (7) can be transformed into the following three master equations for this configuration.

$$\varepsilon_1=\left(\frac{p(1+\lambda\sqrt{w^2+p})e^{-\lambda\sqrt{w^2+p}}}{(1-w)(w^2+p)^{3/2}}\right)^2\left(\frac{(1-w)(w^2+p)}{1+\lambda\sqrt{w^2+p}}+\frac{w((1-w)^2+p)}{1+\lambda\sqrt{(1-w)^2+p}}-\frac{p}{2}\right) \tag{8}$$

$$r=\frac{(1-w)(w^2+p)^{3/2}e^{\lambda\sqrt{w^2+p}}}{p^2(1+\lambda\sqrt{w^2+p})} \tag{9}$$

$$\frac{w(1+\lambda\sqrt{w^2+p})e^{-\lambda\sqrt{w^2+p}}}{(w^2+p)^{3/2}}=\frac{b(1-w)(1+\lambda\sqrt{(1-w)^2+p})e^{-\lambda\sqrt{(1-w)^2+p}}}{((1-w)^2+p)^{3/2}} \tag{10}$$

The quantities ε_1 and *r* now depend only on the coordinates *w* and *p* (besides the constant λ). Therefore, if we solve (10) for *p* and substitute it to (8) and (9), we obtain the parametric solution for the energy terms $\varepsilon_1(r)$ with the parameter *w* for the given *b* and λ.

Equation (10) does not allow an exact analytical solution for *p*. Therefore, we will use an approximate analytical method.

Below is the contour plot of this equation for $b = 3$ and $\lambda = 0.1$.

As in [17], which presented the study of the same *ZeZ'* system for $\lambda = 0$, the plot has two branches, the left one spanning from $w = 0$ to $w = w_1$, and the right one from the asymptote $w = w_3$ to $w = 1$. Here w_1 is a solution of the equation

$$(1-w_1)^2(1+\lambda w_1)e^{\lambda(1-2w_1)}=bw_1^2(1+\lambda(1-2w_1)) \tag{11}$$

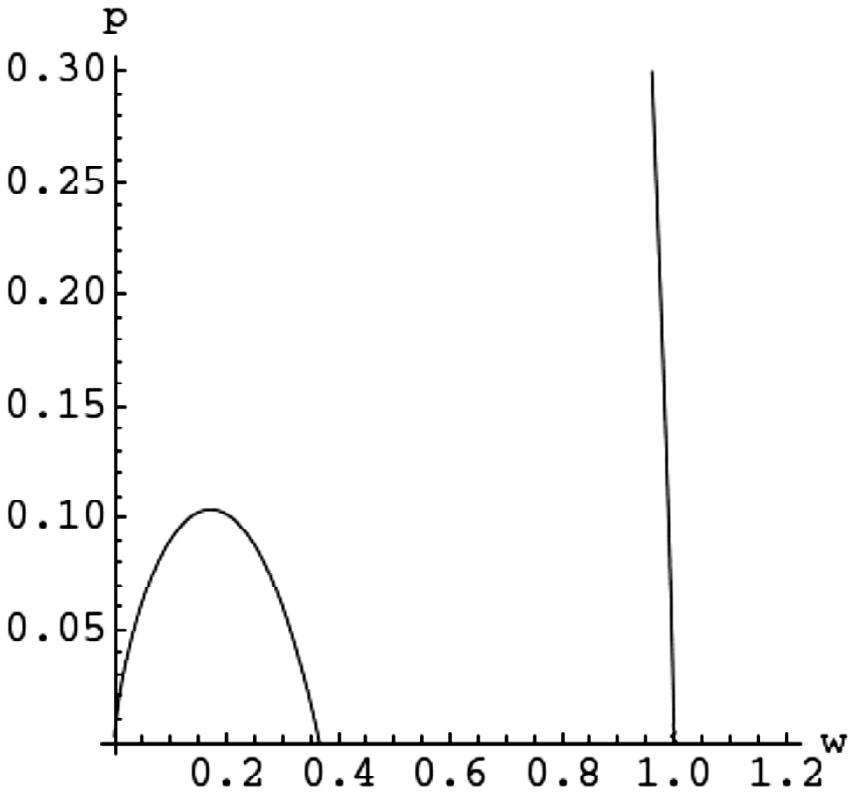

Figure 1: Contour plot of equation (10) for b = 3 and λ = 0.1

in the interval $0 < w_1 < 1$, and w_3 does not depend on λ and equals $b/(1 + b)$ – the same as in [17] for λ = 0. As λ increases, w_1 and the p-coordinate of the maximum of the left branch increase, but the general shape of both curves is preserved. Below is the plot for a relatively strong screening: λ = 2.

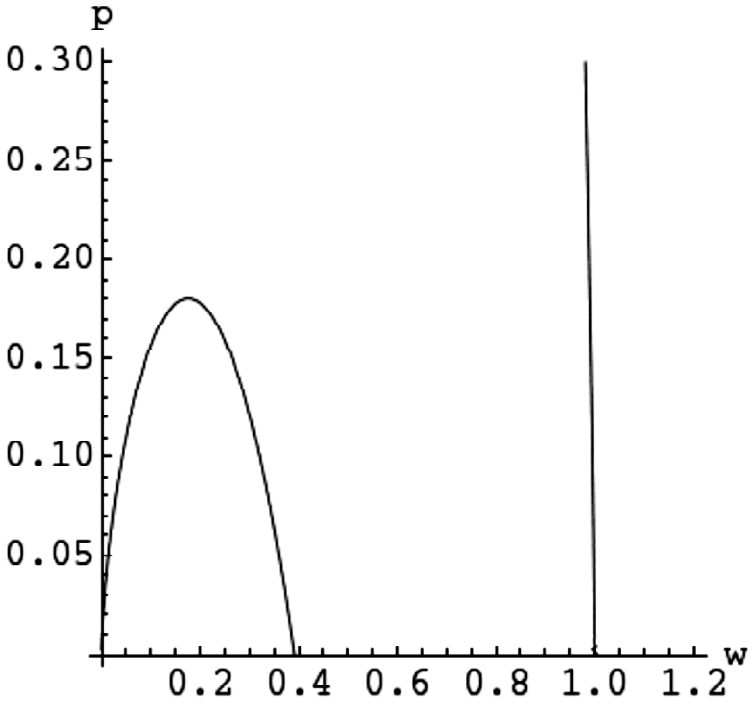

Figure 2: Contour plot of equation (10) for b = 3 and λ = 2

An approximation was made for small values of λ. Approximating (10) in the first power of λ, we obtain the expression involving only the second and higher powers of λ. Therefore, an attempt was made using the value of $p(w)$ for λ = 0 presented in [17], which we shall denote as p_0; it is the same as the squared quantity in equation (11) in [17]. Further, taking the higher powers of λ into account, we obtained the next-order approximation for $p(w)$:

$$p(w) = p_0 + \frac{\lambda^2}{6}(1-2w)\left(1+(1-2w)\left(\frac{w^{2/3}+b^{2/3}(1-w)^{2/3}}{w^{2/3}-b^{2/3}(1-w)^{2/3}}\right)^2\right) \tag{12}$$

where

$$p_0 = \frac{w^{2/3}(1-w)^{4/3}-b^{2/3}w^2}{b^{2/3}-w^{2/3}(1-w)^{-2/3}} \tag{13}$$

– the zero-λ value as in equation (11) in [17].

Equation (11) of the present paper can be approximated by substituting $1 + \lambda(1 - 2w_1)$ in place of $\exp(\lambda(1 - 2w_1))$, which will render it a 4th-degree polynomial in w_1. The analytical expression for it is given in Appendix A.

Substituting (12) into (8) and (9), we obtain the approximate parametric solution for the energy terms $-\varepsilon_1(r)$ by running the parameter w on $0 < w < w_1$ and $w_3 < w < 1$. Empirically, by comparison with the numerical results, it was found that using the value of p from (13) on the $0 < w < w_1$ range and from (12) on the $w_3 < w < 1$ range gives the best approximate results. Below are the approximate classical energy terms for $b = 3$ and different values of λ.

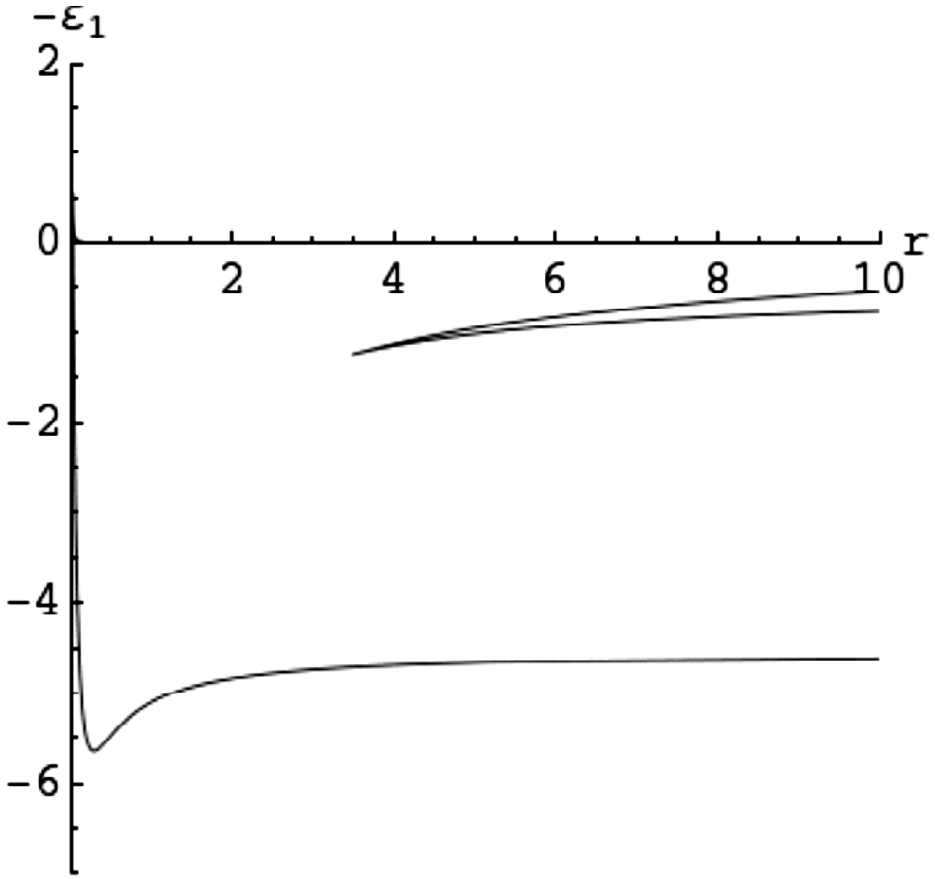

Figure 3: Approximate classical energy terms for $b = 3$ at λ = 0.1

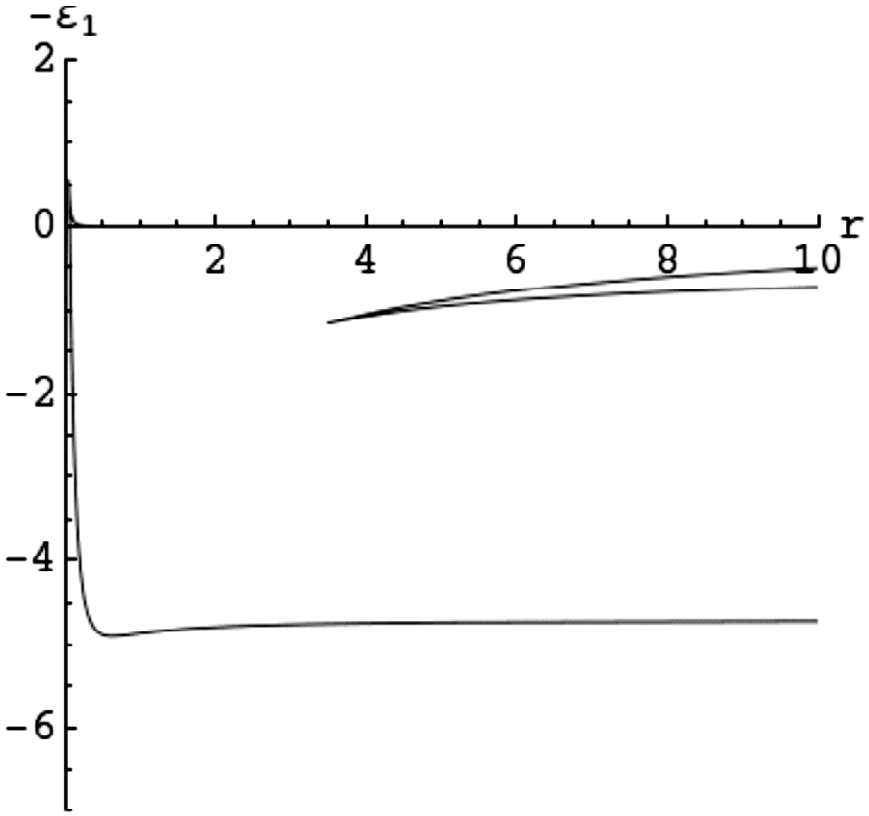

Figure 4: Approximate classical energy terms for b = 3 at λ = 0.2

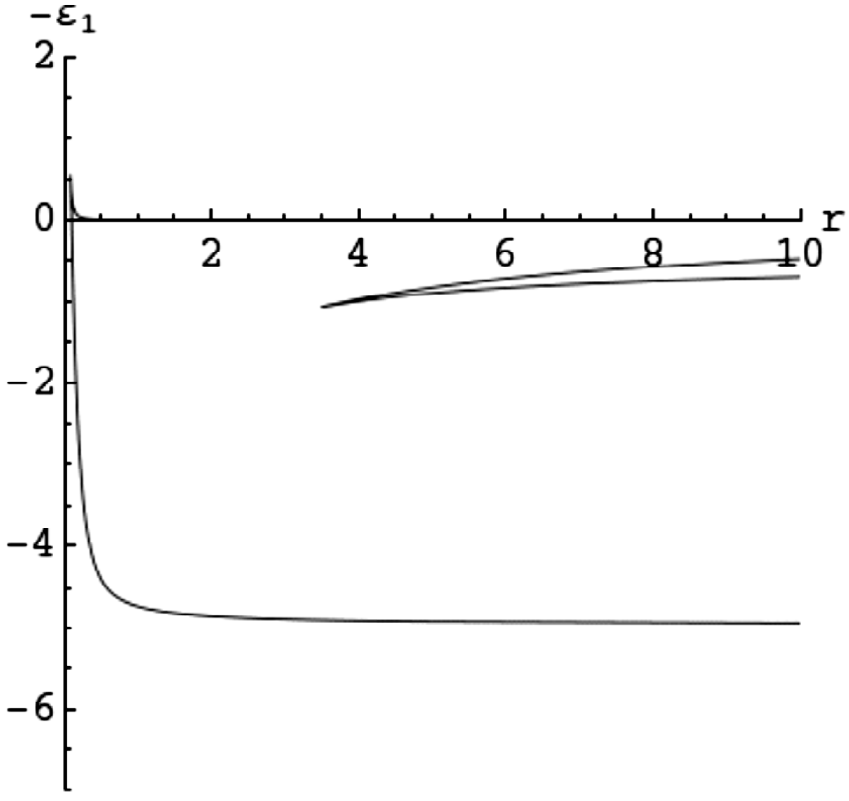

Figure 5: Approximate classical energy terms for b = 3 at λ = 0.3

A numerical solution has also been made. It confirmed that the analytical solution was a good approximation for $\lambda < 0.3$. Below are the terms plotted for selected values of λ.

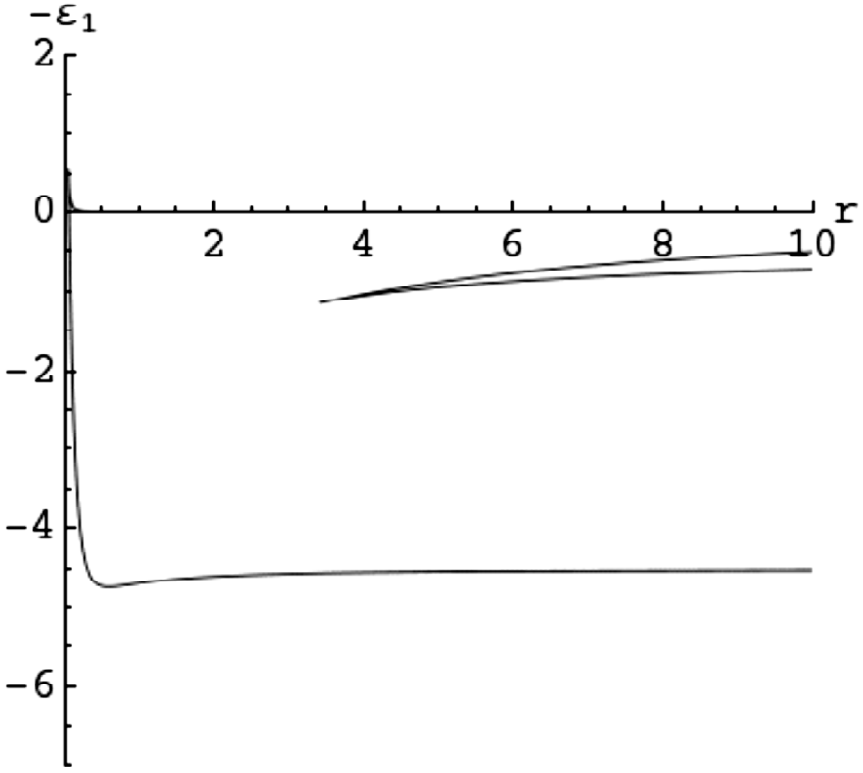

Figure 6: Numerical classical energy terms for b = 3 at λ = 0.2

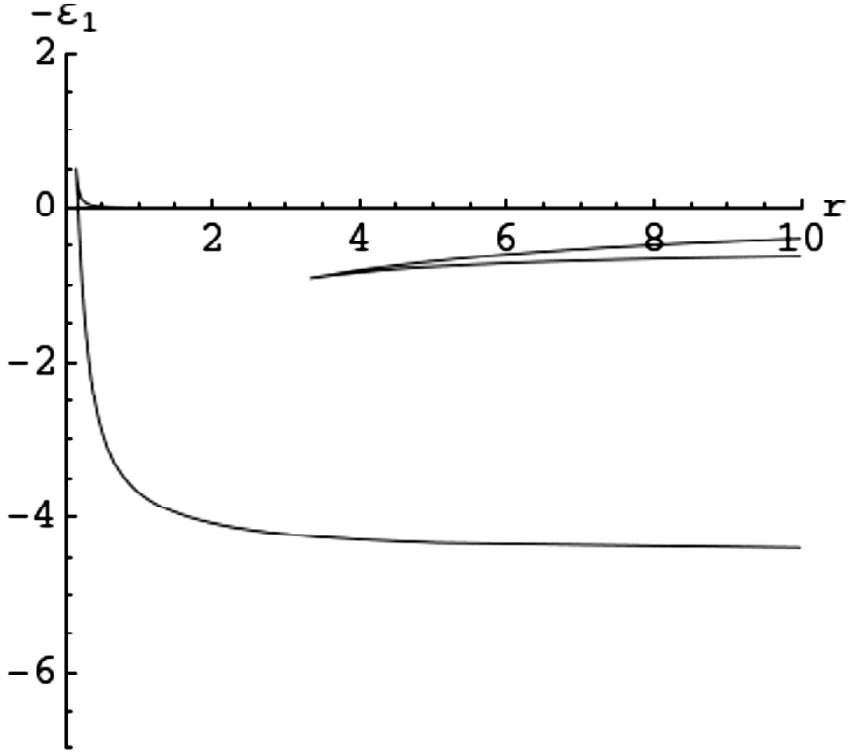

Figure 7: Numerical classical energy terms for b = 3 at λ = 0.5

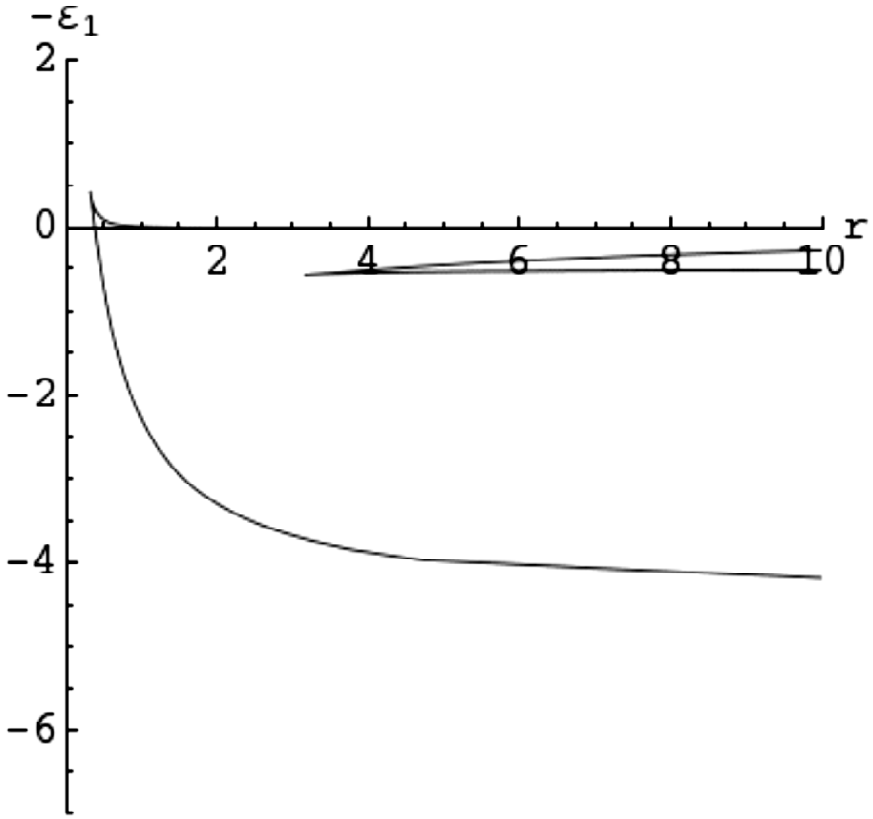

Figure 8: Numerical classical energy terms for b = 3 at λ = 1

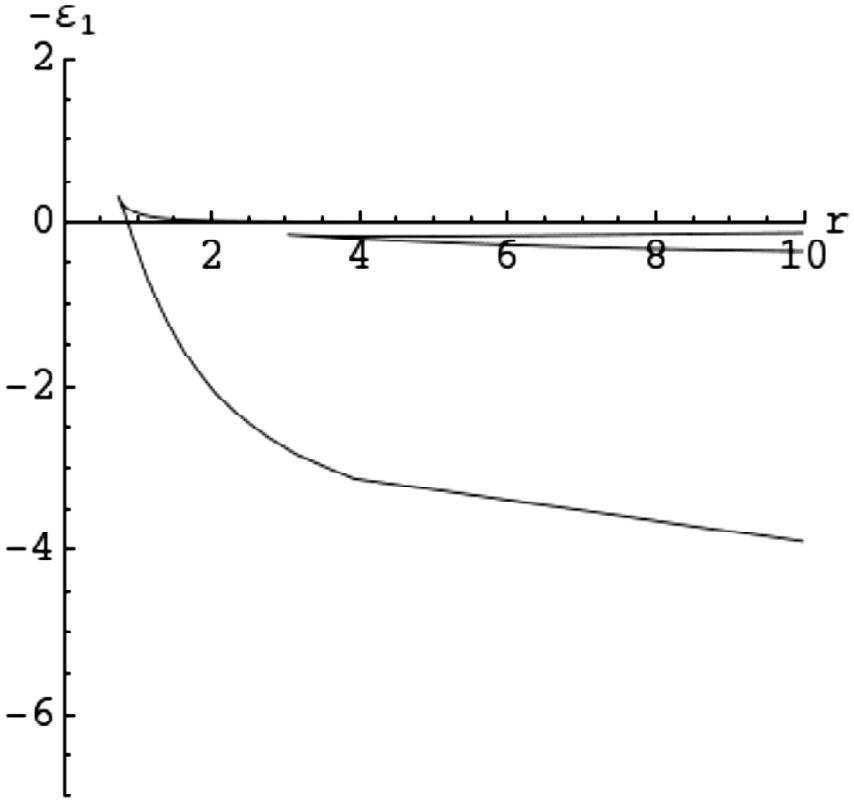

Figure 9: Numerical classical energy terms for b = 3 at λ = 2

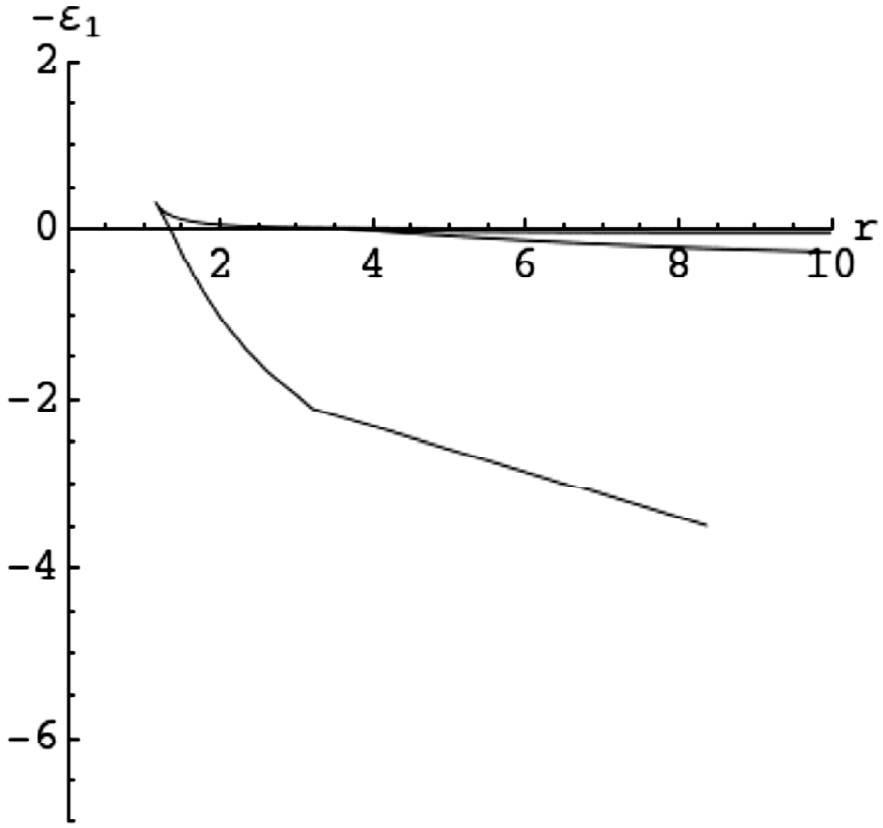

Figure 10: Numerical classical energy terms for b = 3 at λ = 3

The following clarification should be made. The above plots represent "classical energy terms" of the same symmetry. (In physics of diatomic molecules, the terminology "energy terms of the same symmetry" means the energy terms of the same projection of the angular momentum on the internuclear axis.) For a given R and L, the classical energy E takes only several *discrete* values. However, as L varies over a *continuous* set of values, so does the classical energy E (as it should be in classical physics).

3. CROSSINGS OF THE ENERGY TERMS

Several properties of these energy terms have been studied. We note that in case of small or moderate λ, we observe four terms, both pairs of which have a V-type crossing. As an example, we shall take the plot of the terms for λ = 0.2 and number the lowest term 1 and the highest term 2; the remaining terms will be numbered 3 and 4, from the lower one to the higher one. Therefore, terms 1 and 2 and terms 3 and 4 undergo V-type crossings, to which we shall refer as V12 and V34. Using a small-λ approximation by choosing (13) as the $p(w)$ solution for the parametric energy terms (essentially, a zero-λ approximation), we can substitute (13) into (9), which will give it the form below.

$$r = \frac{(1-2w)^{3/2}\sqrt{b^{2/3} - \left(\frac{w}{1-w}\right)^{2/3}}}{w^3\left(b^{2/3} - \left(\frac{1-w}{w}\right)^{4/3}\right)^2} \tag{14}$$

For a given b, the terms 3 and 4 are produced by varying w between 0 and w_1. The V34 crossing occurs at the value of w where $r(w)$ has a minimum [17]. Therefore, setting the derivative dr/dw to zero, we obtain the equation whose solution for w in the range $0 < w < w_1$ gives us the point on the parametric axis which produces the V34 crossing.

$$9w^{4/3}(1-w)^{4/3}(w^{4/3}+b^{4/3}(1-w)^{4/3})=b^{2/3}(1-4w+22w^2-36w^3+18w^4) \tag{15}$$

This equation has no dependence on λ and is therefore equivalent to the Coulomb-potential case (λ = 0). It turns out that the form of the parametric dependence $\varepsilon_1(r)$ in this case can be significantly simplified by introducing a new parameter

$$\gamma=\left(\frac{1}{w}-1\right)^{1/3} \tag{16}$$

In this case, $w = 0$ will correspond to $\gamma = +\infty$ and $w = 1$ will correspond to $\gamma = 0$, thus $\gamma > 0$ in the allowed regions. The points $w_1 = 1/(1 + b^{1/2})$ and $w_3 = b/(1 + b)$ defining the allowed regions $0 < w < w_1$, $w_3 < w < 1$ (here we assume $b > 1$) will correspond to $\gamma_1 = b^{1/6}$ and $\gamma_3 = 1/b^{1/3}$ (notice that $0 < w < w_1$ corresponds to $+\infty > \gamma > \gamma_1$ and $w_3 < w < 1$ corresponds to $\gamma_3 > \gamma > 0$). The energy terms $\varepsilon_1(r)$ for the Coulomb-potential case will take the following parametric form:

$$\varepsilon_1(\gamma,b)=\frac{(b^{2/3}-\gamma^4)^2(\gamma(\gamma^3-2)+b^{2/3}(2\gamma^3-1))}{2(\gamma^3-1)^2(\gamma^6-1)} \tag{17}$$

$$r(\gamma,b)=\frac{\sqrt{b^{2/3}\gamma^2-1}(\gamma^6-1)^{3/2}}{\gamma(b^{2/3}-\gamma^4)^2} \tag{18}$$

The parametric plot of (17) and (18) with the parameter γ varied from 0 to $1/b^{1/3}$ and from $b^{1/6}$ to $+\infty$ for $b = 3$ will yield the same graph as in Fig. 3 in [17].

The crossing of the top two terms corresponds to the point where $r(\gamma, b)$ has a minimum or $\varepsilon_1(\gamma, b)$ has a maximum for a given b. Thus, taking the derivative of either function by γ and setting it equal to zero will yield a solution for the γ on the interval $\gamma > 1$ corresponding to the crossing. The equation for γ obtained from differentiating $r(\gamma)$ is a 6th-power polynomial and cannot be solved analytically; however, the equation for γ obtained from differentiating $\varepsilon_1(\gamma)$ can be solved analytically for γ. Below is the critical value γ_0 corresponding to the crossing.

$$\gamma_0=\sqrt{b^{1/3}+\frac{(b-1)^{1/3}}{b^{1/6}}((\sqrt{b}+1)^{1/3}+(\sqrt{b}-1)^{1/3})} \tag{19}$$

Therefore, an analytical solution exists for (15). Going back to the w-parametrization, we obtain the analytical solution of (15):

$$w_{V34}=\frac{1}{1+\left(b^{1/3}+\frac{(b-1)^{1/3}}{b^{1/6}}((\sqrt{b}+1)^{1/3}+(\sqrt{b}-1)^{1/3})\right)^{3/2}} \tag{20}$$

Substituting it into (9) and using the numerical solution for p of (10), we obtain the semi-analytical dependence $r_{V34}(\lambda)$ for a given b. Below is the plot for $b = 3$.

Since the plot in Fig. 11 was obtained using a zero-λ approximation for the point of the V34 crossing, we also graphed this dependence numerically point by point. The graph below for the same b shows that in relation to terms 3 and 4, this approximation works well even for moderate values of λ.

The energy of the V34 crossing can be obtained semi-analytically by substituting the numerical solution for p of (10) into (8), and by further substituting (20) into the resulting formula. It could be seen that as λ grows, the energy of the crossing grows and at a relatively large λ becomes positive. A numerical graph can also be made in a fashion similar to Fig. 12. A visual comparison shows a good similarity between the two. Below, a numerical graph is given for $b = 3$.

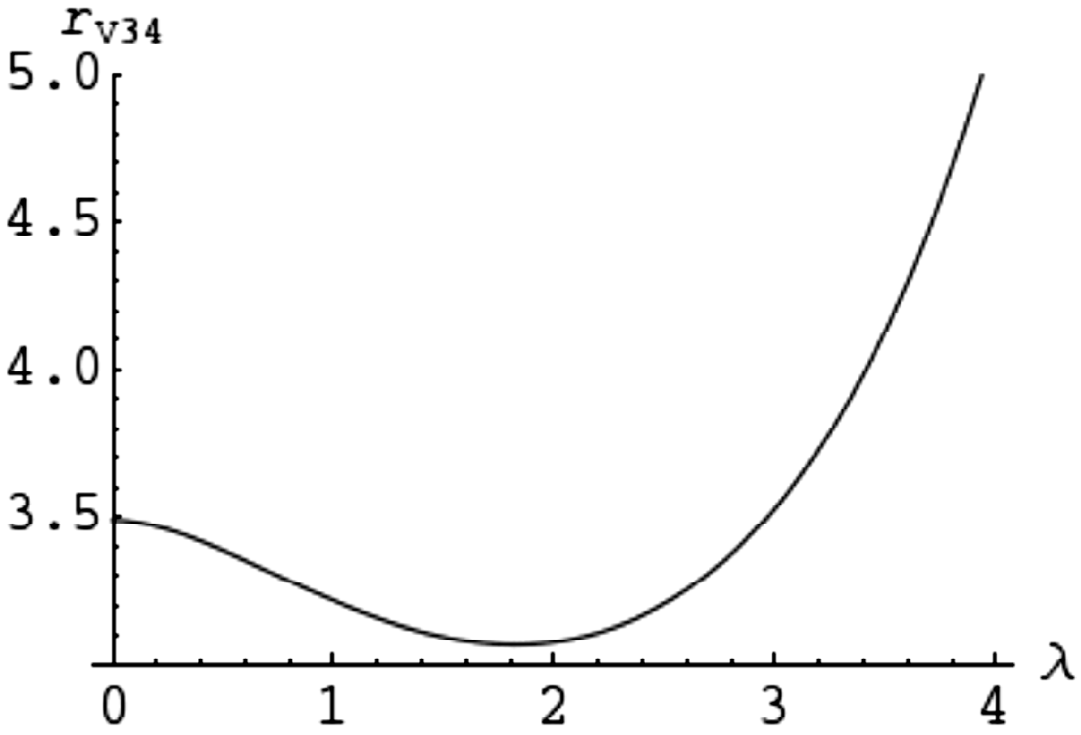

Figure 11: Semi-analytical plot of $r_{V34}(\lambda)$ for b = 3

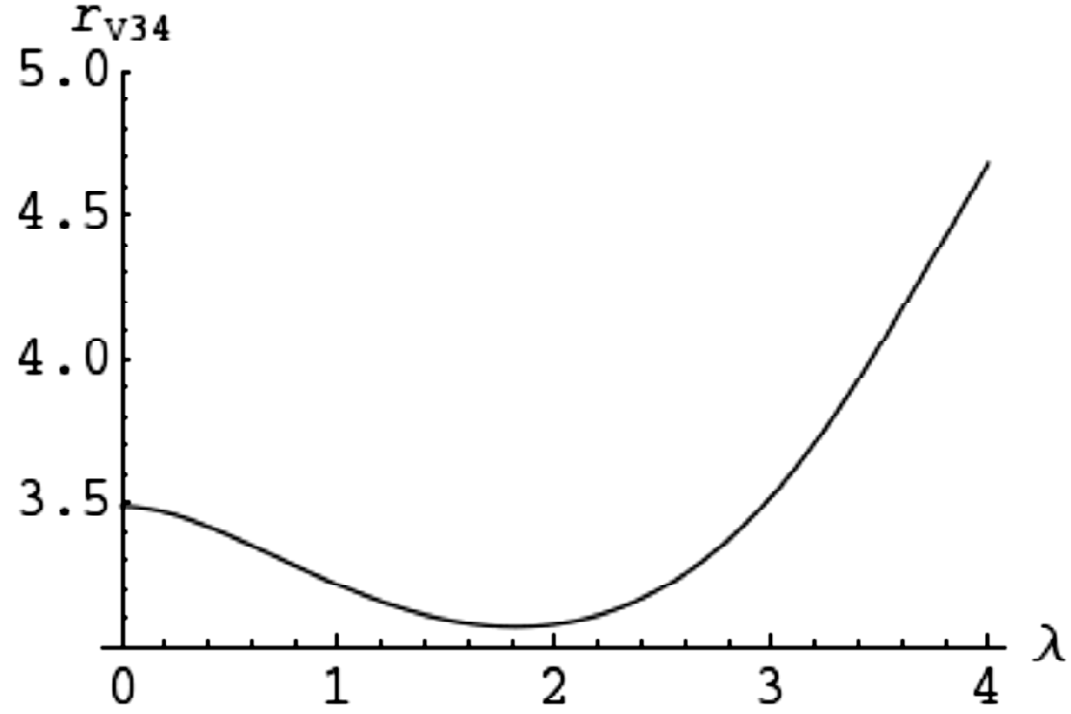

Figure 12: Numerical plot of $r_{V34}(\lambda)$ for b = 3

As we see, the energy of the V34 crossing becomes positive after λ = 2.96, has a maximum, and later asymptotically approaches zero. For b = 4/3, the V34 crossing reaches zero energy at λ = 2.13.

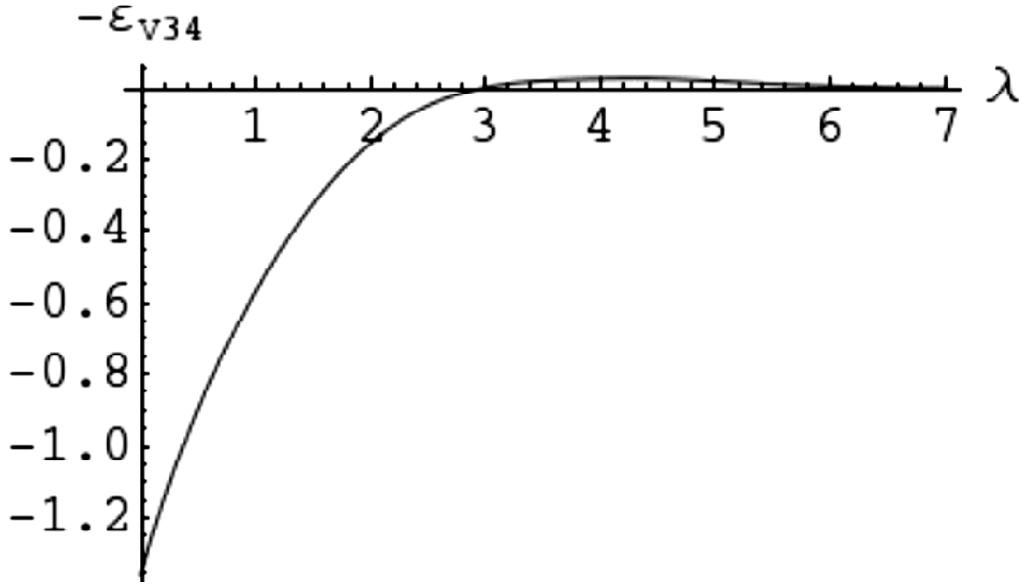

Figure 13: Numerical plot of $-\varepsilon_{V34}(\lambda)$ for $b = 3$

The shape of the terms 3 and 4 is also affected by the screening. Term 3, whose energy increases as r increases, becomes nearly horizontal at energy –0.5 at a certain value of λ; at further λ, its energy decreases with r. For $b = 3$, this value of λ is about 1.1; for $b = 4/3$, it is about 0.7. The plots are shown below.

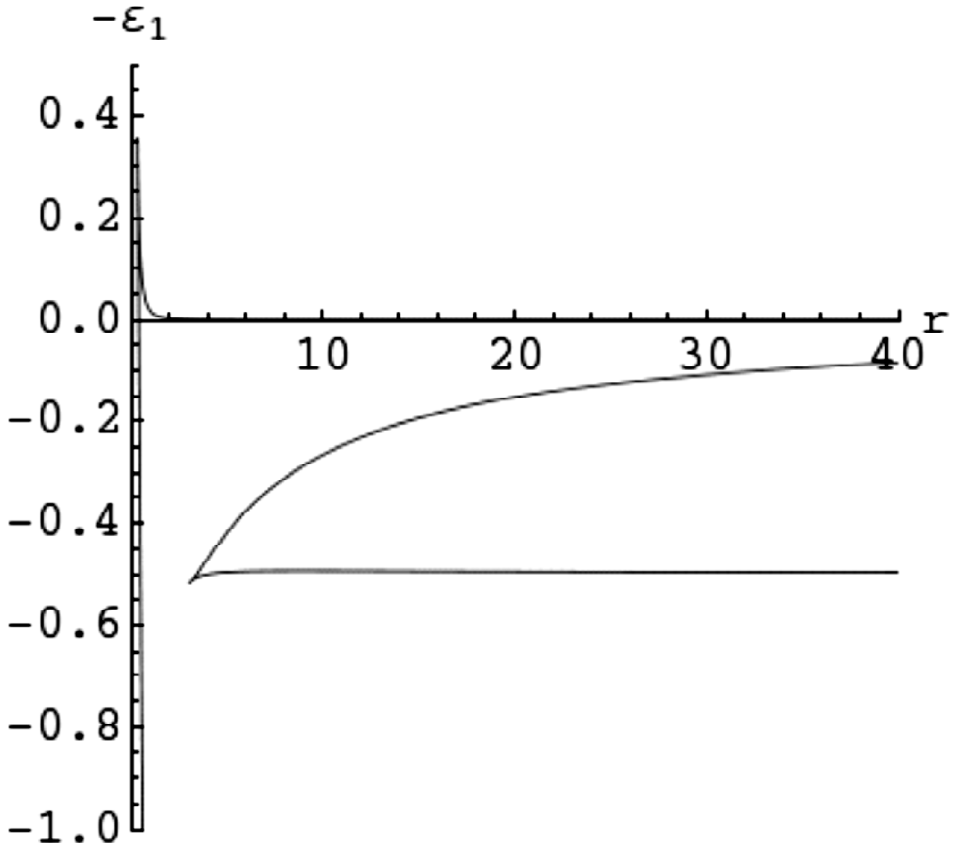

Figure 14: Classical energy terms for $b = 3$ at $\lambda = 1.1$; term 3 is nearly constant at energy $-\varepsilon_1 = -0.5$

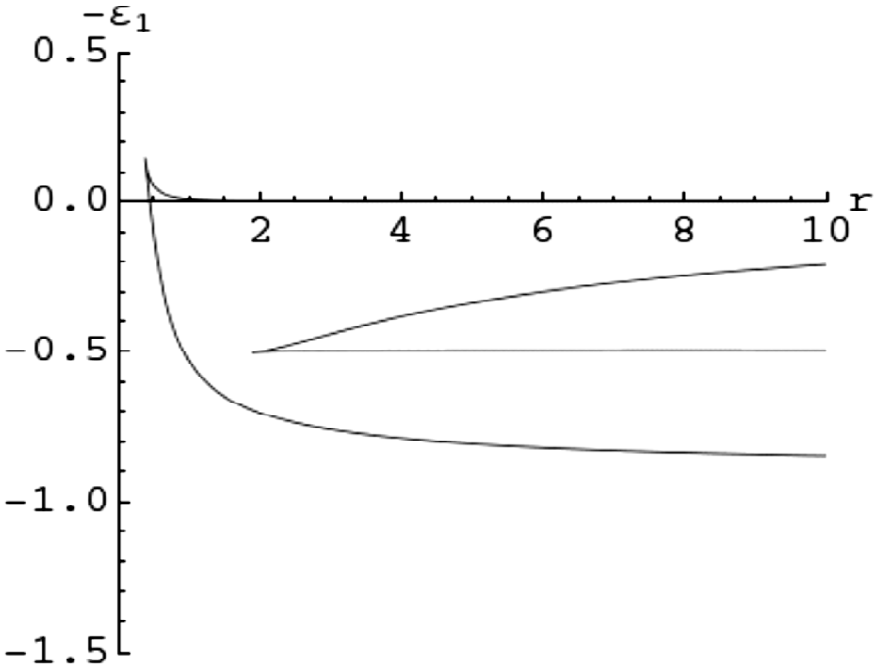

Figure 15: The same as Fig. 14, but for b = 4/3 at λ = 0.7

For V12 crossing, the small-λ approximation is not applicable since this crossing is not observed at λ = 0. Therefore, only numerical methods were used. A situation of particular interest is the behavior of term 1 at very small r, because as $r \to 0$ it corresponds to the energy of the hydrogenic ion of the nuclear charge $Z + Z'$ [8]. The point with the smallest r is the V12 crossing. A comparison was made of the dependence of the electronic energy on the screening parameter λ between [8] and the limiting case $r \to 0$ in our situation. Since in the paper mentioned above, the calculation was performed for a single Coulomb center Z, we had to re-scale the quantities to make a valid comparison. The electronic energies are related as $\varepsilon_1^{(TCC)} = (1 + b)^2 \varepsilon_1^{(OCC)}$, where OCC stands for "one Coulomb center". Since the scaling for the screening parameter in the OCC case did not include R (the internuclear distance), the scaling factor between the screening parameter includes r: $\lambda^{(TCC)} = r(1 + b)\, \lambda^{(OCC)}$. Taking this into account, we can plot the energy dependence on λ for the limiting case $r \to 0$.

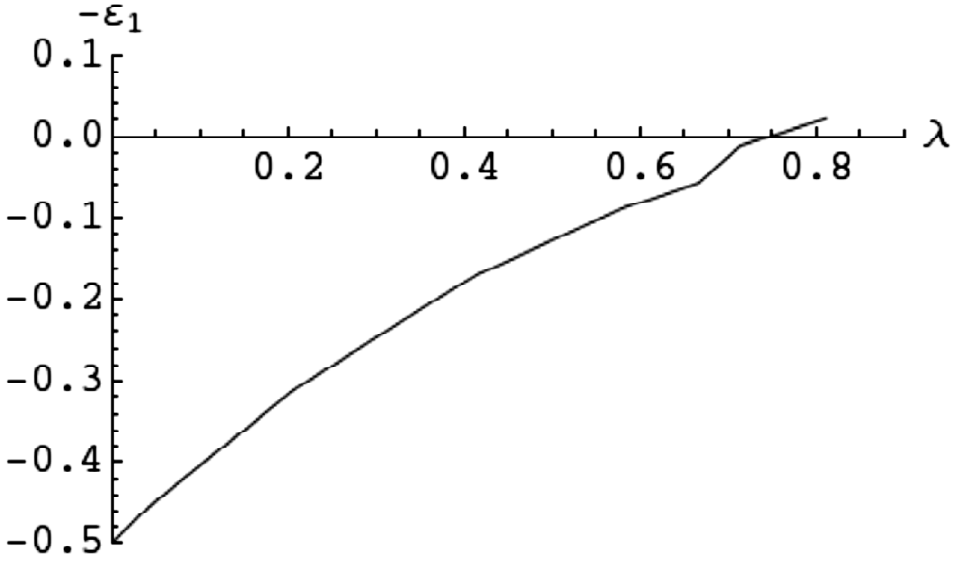

Figure 16: Plot of the energy of the electron versus the scaled screening factor for b = 3 in the limit $r \to 0$

Below is the dependence obtained in [8] for OCC:

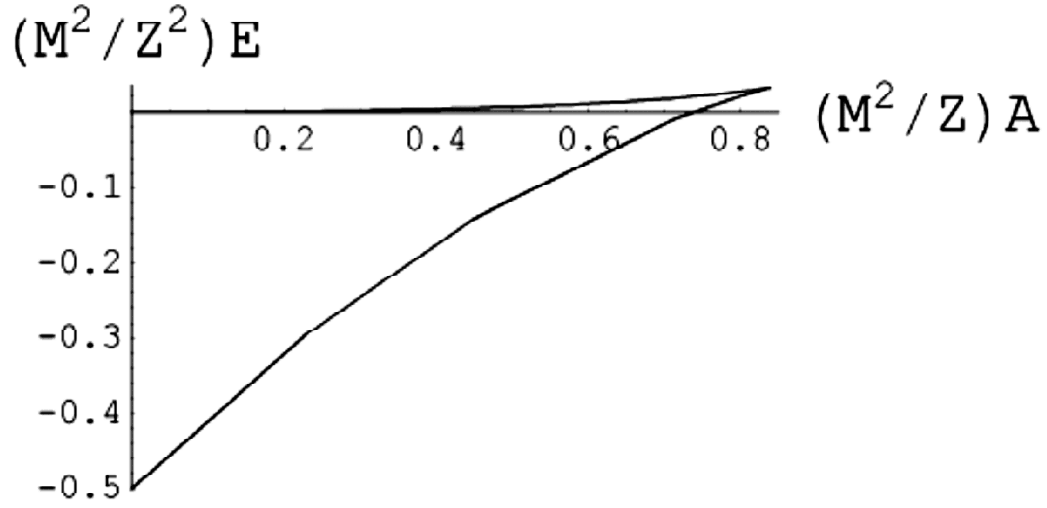

Figure 17: Plot of the energy of the electron in a OCC system versus the scaled screening factor

4. THE EFFECT OF THE PLASMA SCREENING ON THE INTERNUCLEAR POTENTIAL

Another aspect of this problem worth studying is the internuclear potential. Previously its properties were studied for the same system with $\lambda = 0$ and a magnetic field parallel to the internuclear axis [8]. Particularly, the magnetic field created a deep minimum in the internuclear potential, which stabilized the nuclear motion and transformed a Rydberg quasi-molecule into a real molecule. Here we shall investigate the effect of the screening on the internuclear potential. Its form in atomic units is

$$U_{\text{int}} = \frac{ZZ'}{R} + E \tag{21}$$

where E is the electronic energy. Using the scaled quantities from (4), we have the scaled internuclear potential

$$u_{\text{int}} = \frac{bZ}{r} - \varepsilon_1 \tag{22}$$

where $U_{\text{int}} = (Z/L)^2 u_{\text{int}}$. By plotting its dependence on r, we found out that in cases of $Z > 1$ the screening tends to flatten the minimum, producing the effect opposite to the one of the magnetic field. Compare the plots of $u_{\text{int}}(r)$ in the case of $Z = 2$, $b = 2$ for $\lambda = 0$ and $\lambda = 0.3$.

The screening increases the potential of the point of intersection of the two branches; the upper branch, which has a very shallow minimum at $\lambda = 0$, loses it as γ increases.

A completely different behavior was observed for $Z = 1$. A small λ creates a deep minimum in the upper branch of the potential. For comparison, we present the plots of the potential in the case of $Z = 1$, $b = 2$ for $\lambda = 0$ and $\lambda = 0.3$.

The figures above reveal the case of the screening stabilization of the nuclear motion for the case of $Z = 1$ and destabilization for $Z > 1$.

5. THE EFFECT OF THE PLASMA SCREENING ON THE CONTINUUM LOWERING

Our analysis of the stability of the electronic motion shows results similar to those obtained by one of us previously in [16,17]. Namely, term 3 corresponds to a stable motion while term 4 – to an unstable motion. So, the crossing point of terms 3 and 4 corresponds to the transition from the stable motion to the unstable motion, leading the electron to the zero energy (i.e., to the free motion) along term 4, which constitutes the ionization of the molecule.

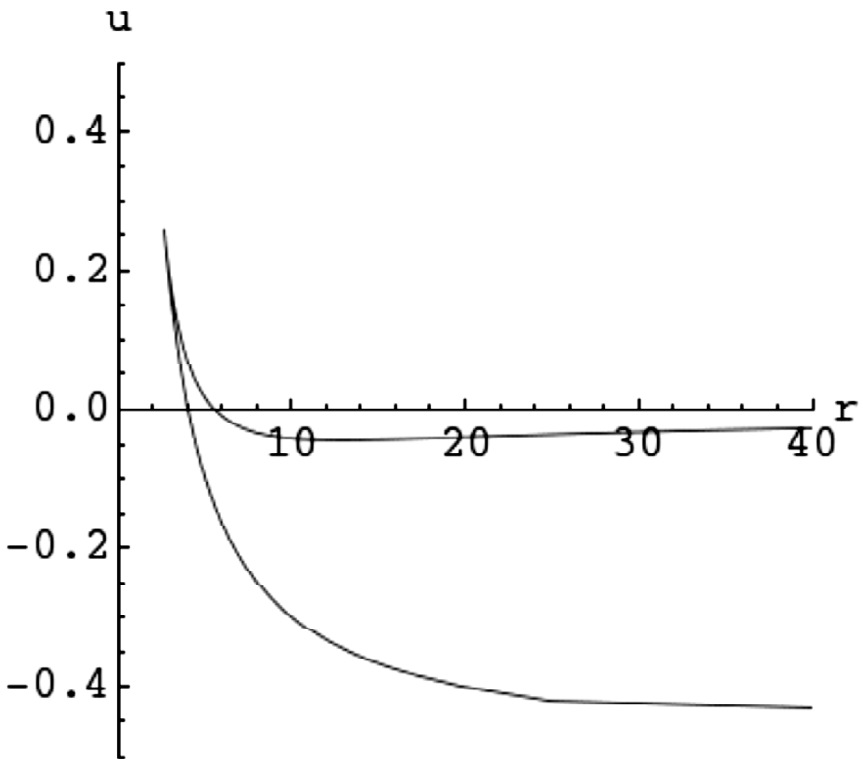

Figure 18: The plot of the scaled internuclear potential versus the scaled internuclear distance for $Z = 2$, $Z' = 4$, $\lambda = 0$

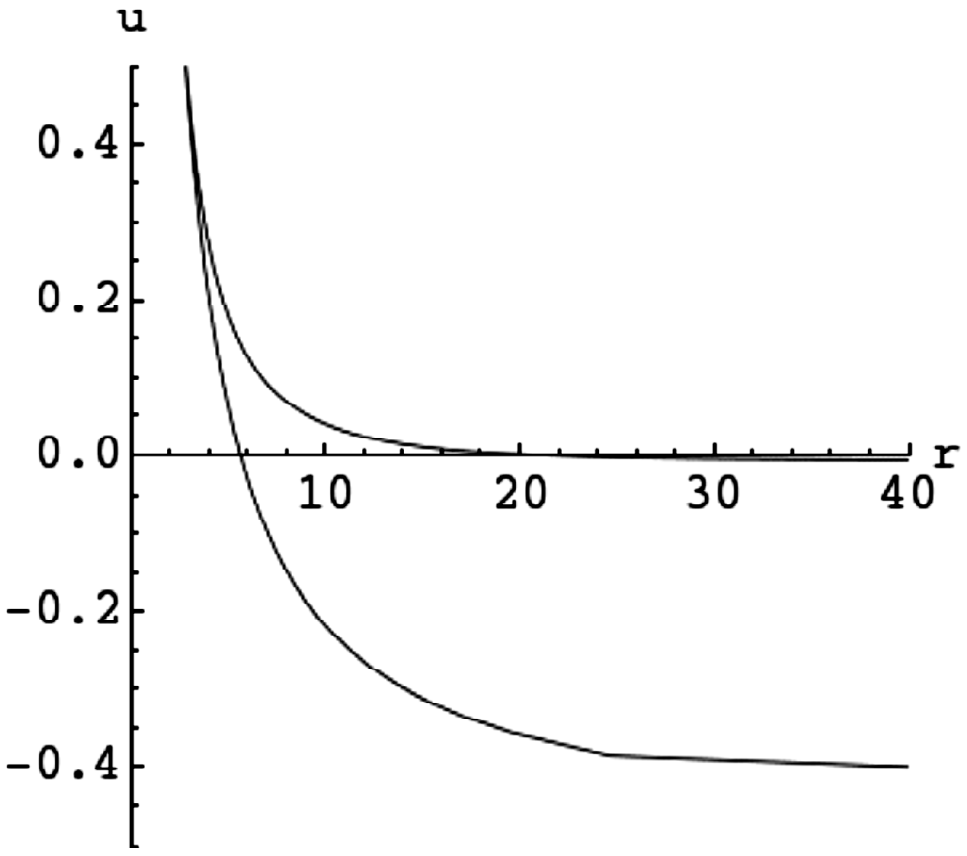

Figure 19: The plot of the scaled internuclear potential versus the scaled internuclear distance for $Z = 2$, $Z' = 4$, $\lambda = 0.3$

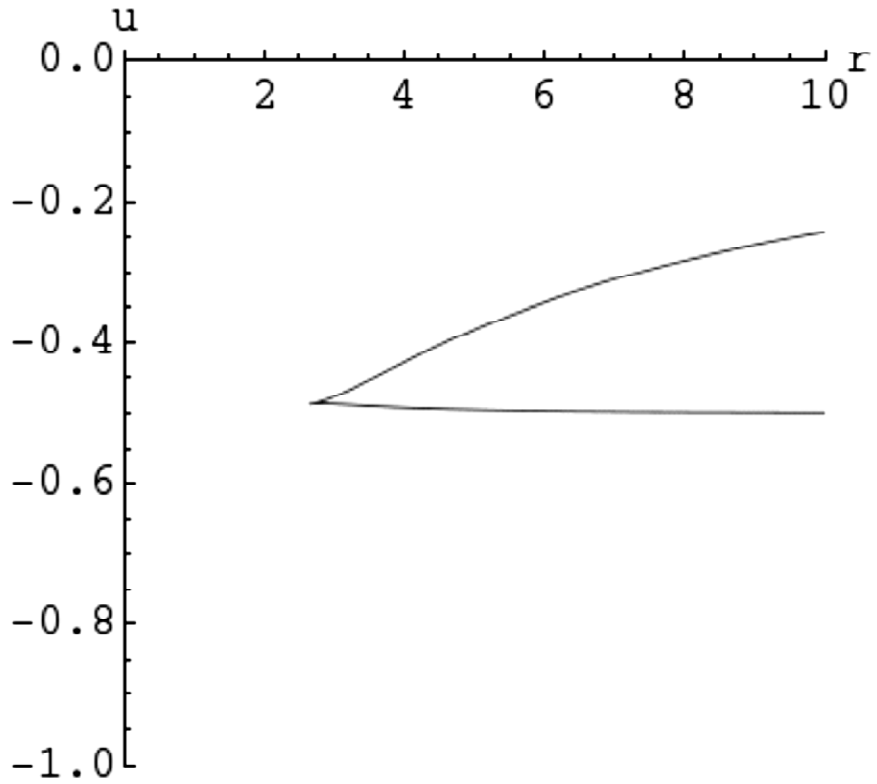

Figure 20: The plot of the scaled internuclear potential versusthe scaled internuclear distance for Z = 1, Z' = 2, λ = 0

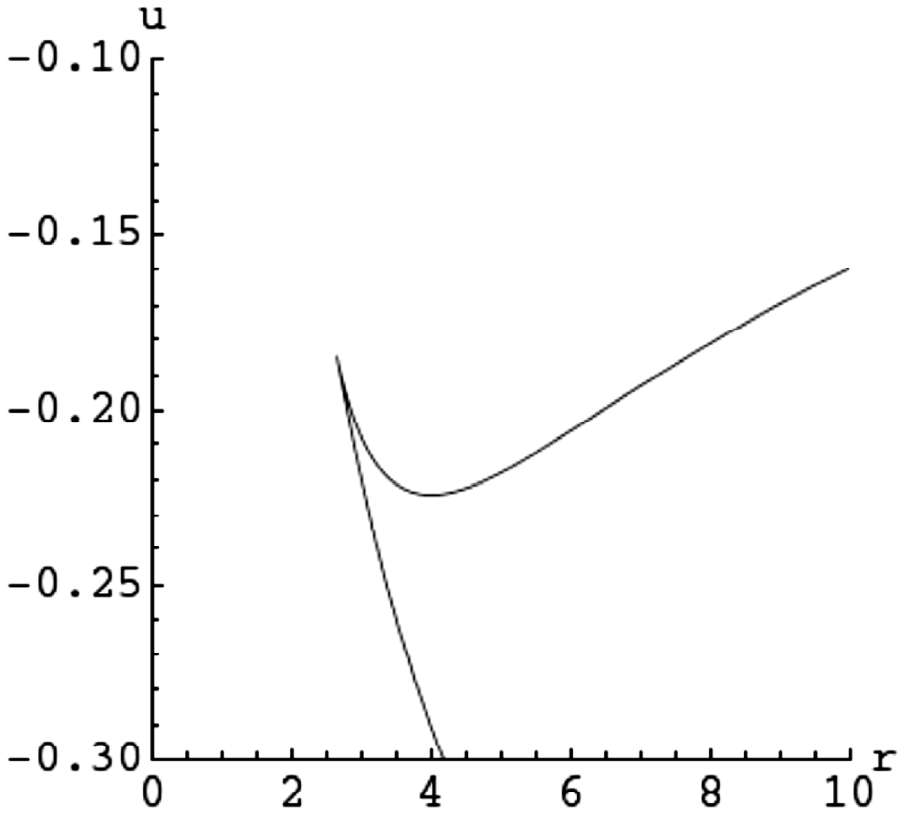

Figure 21: The plot of the scaled internuclear potential versus the scaled internuclear distance for Z = 1, Z' = 2, λ = 0.3

Therefore, we arrive at the following. For the ionization of the hydrogen like ion of the nuclear charge Z_{min} perturbed by the charge Z_{max}, it is sufficient to reach the scaled energy $\varepsilon_c(b) = \varepsilon(w_{V34}(b), b) < 0$. At that point, the electron switches to the unstable motion and the radius of its orbit increases without a limit. This constitutes CL by the amount of $Z < 1 / R > | \varepsilon(w_{V34}(b), b) |$, where $< 1 / R >$ is the value of the inverse distance of the nearest neighbor ion from the radiating ion averaged over the ensemble of perturbing ions.

Thus, CL in the ionization channel is controlled by the scaled energy ε at the crossing point w_{V34} of terms 3 and 4.

The CL for the "default" (λ = 0) TCC system was studied in [30]. Particularly, the scaled CL energy $\varepsilon_c(b) = \varepsilon(w_{V34}(b), b) = \Delta E/(Z<1/R>)$ was graphed on a double-logarithmic scale, where ε is defined in (4) and w_{V34} is given by (16). The graph is given below; "lg x" stands for "$\log_{10} x$".

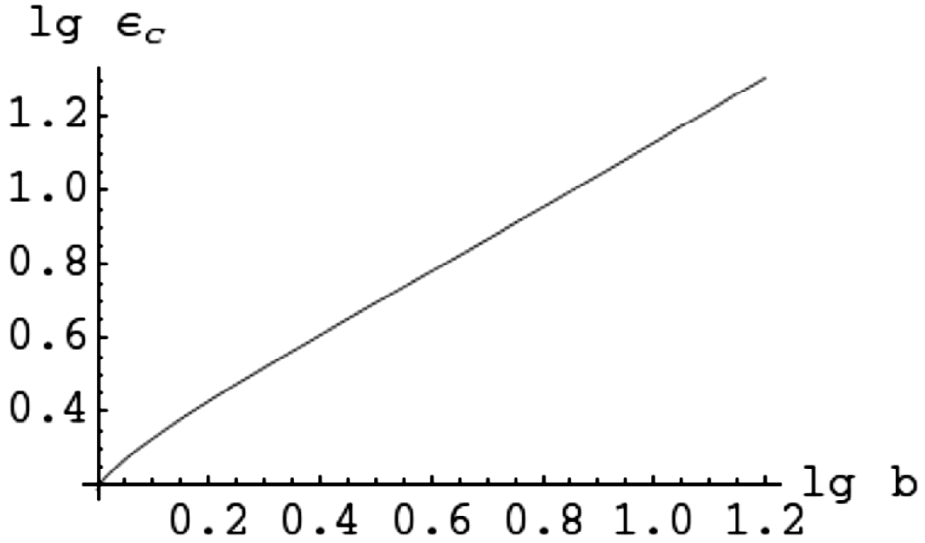

Figure 22: The plot of the CL energy versus *b* on a double logarithmic scale for λ = 0

We have made several plots of $\varepsilon_c(b)$ for several values of λ. A numerical value for w_{V34} was taken to increase precision.

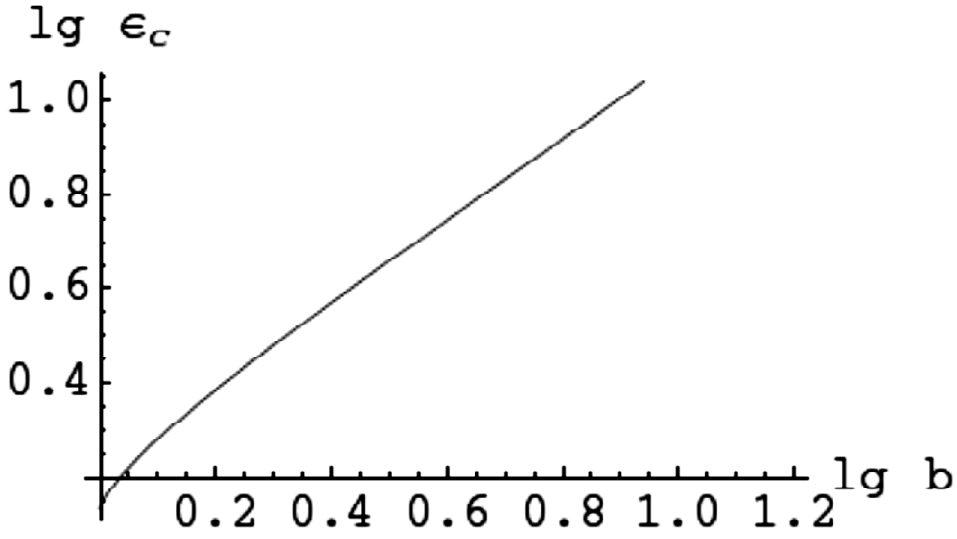

Figure 23: The plot of the CL energy versus *b* on a double logarithmic scale for λ = 0.1

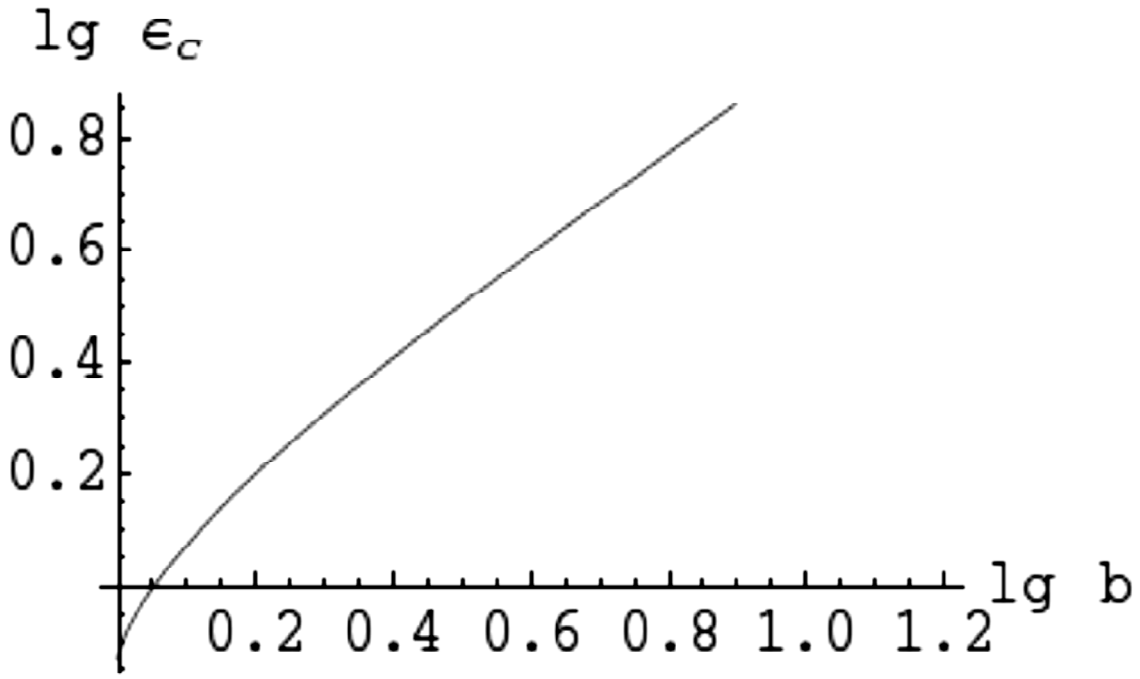

Figure 24: The plot of the CL energy versus *b* on a double logarithmic scale for λ = 0.5

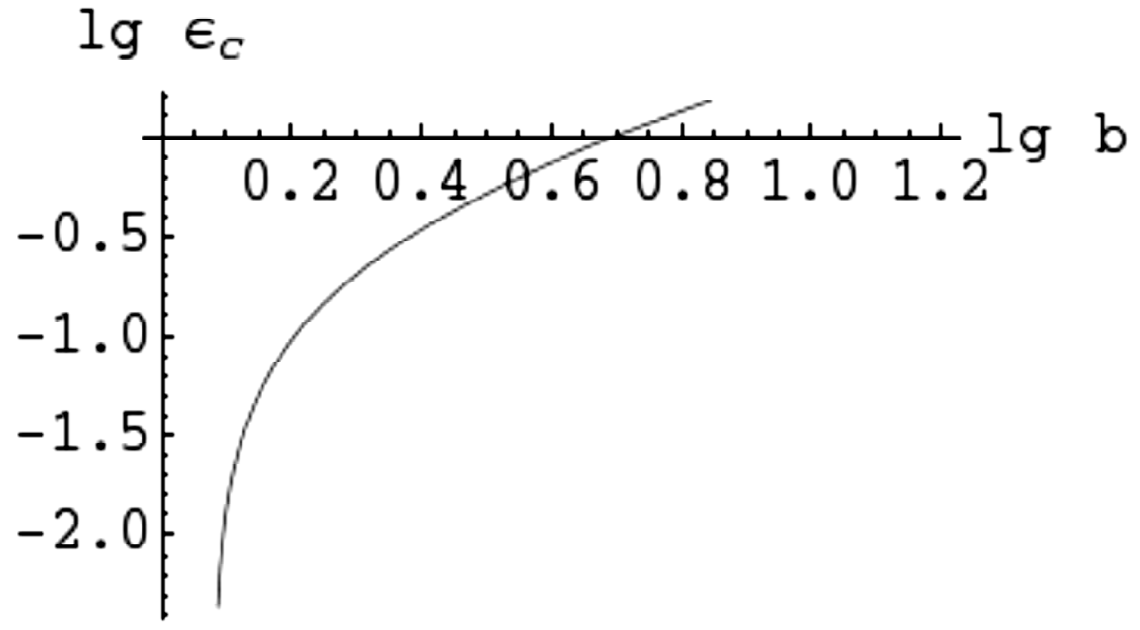

Figure 25: The plot of the CL energy versus *b* on a double logarithmic scale for λ = 2

From the figures above we can see that the plasma screening decreases the value of the CL in the ionization channel. Also, starting from about λ = 1.7, we observe the "cutoff" value of $b > 1$, below which ε_c becomes negative, i.e., the electron energy at w_{V34} becomes positive. This means that there is no more CL in this ionization channel – instead, the continuum becomes higher than for the isolated hydrogen-like ion of the nuclear charge *Z*. This effect cannot be observed in the logarithmic graphs above because the cutoff value of energy (zero) corresponds to $\lg \varepsilon_c = -\infty$. Below we made the standard, non-logarithmic plots of $\varepsilon_c(b)$ for selected values of λ at which this effect is observed.

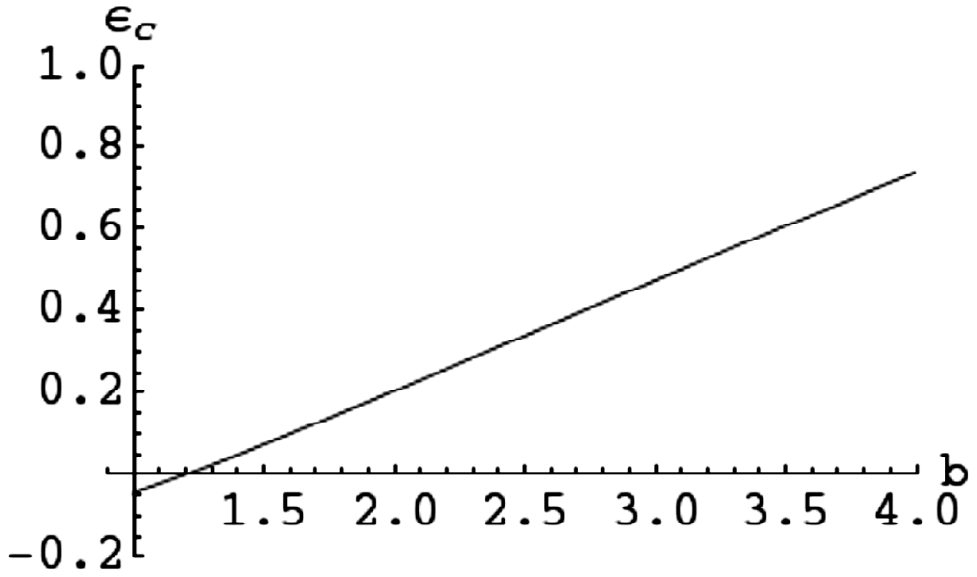

Figure 26: The plot of the CL energy versus *b* for λ = 2

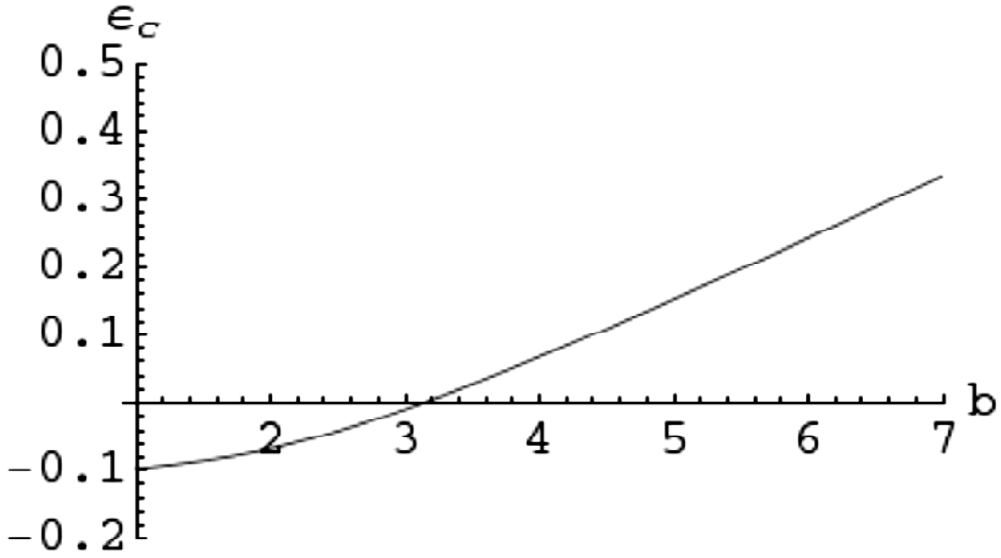

Figure 27: The plot of the CL energy versus *b* for λ = 3

In Fig. 27 we can see that there is no CL for $b = 2$ and $b = 3$ at $\lambda = 3$; the CL starts from $b = 3.2$.

6. CONCLUSIONS

We studied the effects of the plasma screening on the classical energy terms of the electron in the field of two Coulomb centers. We provided analytical results for the small values of the screening factor and numerical results for the medium values.

We found that the plasma screening leads to the appearance of the fourth energy term – in addition to the three classical energy terms with no screening. This term exhibits a V-type crossing with the lowest energy term. The two highest energy terms continue having a V-type crossing like at the zero field.

We studied the effect of the screening on the internuclear potential. We found that the nuclear motion was stabilized by screening for $Z = 1$ and destabilized for $Z > 1$.

The effect of the screening on the continuum lowering was studied as well. The plasma screening decreases the value of the CL in the ionization channel, similar to the effect of the magnetic field [11].

Appendix A
The analytical expression for the limit w_1 in Eq. (11) in the small-λ approximation

$$
-\frac{-b-5\lambda+1}{8\lambda}-\frac{1}{2}\sqrt{\left(\frac{(-b-5\lambda+1)^2}{16\lambda^2}-\frac{4\lambda^2+b\lambda-3\lambda+b-1}{3\lambda^2}+\frac{1}{6\sqrt[3]{2}\,\lambda^2}\right.}
$$

$$
\left(\left(2\left(4\lambda^2+b\lambda-3\lambda+b-1\right)^3-144(-\lambda-1)\lambda^2\left(4\lambda^2+b\lambda-3\lambda+b-1\right)-\right.\right.
$$

$$
9\left(-5\lambda^2-b\lambda+\lambda\right)\left(-\lambda^2+3\lambda+2\right)\left(4\lambda^2+b\lambda-3\lambda+b-1\right)+
$$

$$
27(-\lambda-1)\left(-5\lambda^2-b\lambda+\lambda\right)^2+54\lambda^2\left(-\lambda^2+3\lambda+2\right)^2+
$$

$$
\sqrt{\left(\left(2\left(4\lambda^2+b\lambda-3\lambda+b-1\right)^3-144(-\lambda-1)\lambda^2\left(4\lambda^2+b\lambda-3\lambda+b-1\right)-\right.\right.}
$$

$$
9\left(-5\lambda^2-b\lambda+\lambda\right)\left(-\lambda^2+3\lambda+2\right)\left(4\lambda^2+b\lambda-3\lambda+b-1\right)+
$$

$$
27(-\lambda-1)\left(-5\lambda^2-b\lambda+\lambda\right)^2+54\lambda^2\left(-\lambda^2+3\lambda+2\right)^2\Big)^2-
$$

$$
\left.\left.4\left(\lambda^4+5b\lambda^3+b^2\lambda^2+11b\lambda^2-2\lambda^2+2b^2\lambda-2b\lambda+\right.\right.\right.
$$

$$
\left.\left.\left.b^2-2b+1\right)^3\right)\Big)\,\hat{}\,(1/3)\Big)+
$$

$$
\left(\lambda^4+5b\lambda^3+b^2\lambda^2+11b\lambda^2-2\lambda^2+2b^2\lambda-2b\lambda+b^2-2b+1\right)/
$$

$$
\left(3\,2^{2/3}\lambda^2\left(2\left(4\lambda^2+b\lambda-3\lambda+b-1\right)^3-144(-\lambda-1)\lambda^2\left(4\lambda^2+b\lambda-3\lambda+b-1\right)-\right.\right.
$$

$$
9\left(-5\lambda^2-b\lambda+\lambda\right)\left(-\lambda^2+3\lambda+2\right)\left(4\lambda^2+b\lambda-3\lambda+b-1\right)+
$$

$$
27(-\lambda-1)\left(-5\lambda^2-b\lambda+\lambda\right)^2+54\lambda^2\left(-\lambda^2+3\lambda+2\right)^2+
$$

$$
\sqrt{\left(\left(2\left(4\lambda^2+b\lambda-3\lambda+b-1\right)^3-144(-\lambda-1)\lambda^2\left(4\lambda^2+b\lambda-3\lambda+\right.\right.\right.}
$$

$$
\left.\left.b-1\right)-9\left(-5\lambda^2-b\lambda+\lambda\right)\left(-\lambda^2+3\lambda+2\right)\right.
$$

$$
\left(4\lambda^2+b\lambda-3\lambda+b-1\right)+27(-\lambda-1)\left(-5\lambda^2-b\lambda+\lambda\right)^2+
$$

$$
54\lambda^2\left(-\lambda^2+3\lambda+2\right)^2\Big)^2-4\left(\lambda^4+5b\lambda^3+b^2\lambda^2+11b\lambda^2-\right.
$$

$$
\left.\left.\left.2\lambda^2+2b^2\lambda-2b\lambda+b^2-2b+1\right)^3\right)\Big)\,\hat{}\,(1/3)\Big)\right)+
$$

$$
\frac{1}{2}\sqrt{\left(\frac{(-b-5\lambda+1)^2}{8\lambda^2}-\frac{2(4\lambda^2+b\lambda-3\lambda+b-1)}{3\lambda^2}-\frac{1}{6\sqrt[3]{2}\,\lambda^2}\right.}
$$

$$
\left(\left(2\left(4\lambda^2+b\lambda-3\lambda+b-1\right)^3-144(-\lambda-1)\lambda^2\left(4\lambda^2+b\lambda-3\lambda+b-1\right)-\right.\right.
$$

$$9\left(-5\lambda^2-b\lambda+\lambda\right)\left(-\lambda^2+3\lambda+2\right)\left(4\lambda^2+b\lambda-3\lambda+b-1\right)+$$
$$27\left(-\lambda-1\right)\left(-5\lambda^2-b\lambda+\lambda\right)^2+54\lambda^2\left(-\lambda^2+3\lambda+2\right)^2+$$
$$\sqrt{\left(\left(2\left(4\lambda^2+b\lambda-3\lambda+b-1\right)^3-144\left(-\lambda-1\right)\lambda^2\left(4\lambda^2+b\lambda-3\lambda+b-1\right)-\right.\right.}$$
$$9\left(-5\lambda^2-b\lambda+\lambda\right)\left(-\lambda^2+3\lambda+2\right)\left(4\lambda^2+b\lambda-3\lambda+b-1\right)+$$
$$\left.\left.27\left(-\lambda-1\right)\left(-5\lambda^2-b\lambda+\lambda\right)^2+54\lambda^2\left(-\lambda^2+3\lambda+2\right)^2\right)^2-\right.$$
$$4\left(\lambda^4+5b\lambda^3+b^2\lambda^2+11b\lambda^2-2\lambda^2+2b^2\lambda-2b\lambda+\right.$$
$$\left.\left.b^2-2b+1\right)^3\right)\left)\wedge(1/3)\right)-$$
$$\left(\lambda^4+5b\lambda^3+b^2\lambda^2+11b\lambda^2-2\lambda^2+2b^2\lambda-2b\lambda+b^2-2b+1\right)/$$
$$\left(3\,2^{2/3}\lambda^2\left(2\left(4\lambda^2+b\lambda-3\lambda+b-1\right)^3-144\left(-\lambda-1\right)\lambda^2\left(4\lambda^2+b\lambda-3\lambda+b-1\right)-\right.\right.$$
$$9\left(-5\lambda^2-b\lambda+\lambda\right)\left(-\lambda^2+3\lambda+2\right)\left(4\lambda^2+b\lambda-3\lambda+b-1\right)+$$
$$27\left(-\lambda-1\right)\left(-5\lambda^2-b\lambda+\lambda\right)^2+54\lambda^2\left(-\lambda^2+3\lambda+2\right)^2+$$
$$\sqrt{\left(\left(2\left(4\lambda^2+b\lambda-3\lambda+b-1\right)^3-144\left(-\lambda-1\right)\lambda^2\left(4\lambda^2+b\lambda-3\lambda+\right.\right.\right.}$$
$$\left.b-1\right)-9\left(-5\lambda^2-b\lambda+\lambda\right)\left(-\lambda^2+3\lambda+2\right)$$
$$\left(4\lambda^2+b\lambda-3\lambda+b-1\right)+27\left(-\lambda-1\right)\left(-5\lambda^2-b\lambda+\lambda\right)^2+$$
$$54\lambda^2\left(-\lambda^2+3\lambda+2\right)^2\left)^2-4\left(\lambda^4+5b\lambda^3+b^2\lambda^2+\right.\right.$$
$$\left.\left.11b\lambda^2-2\lambda^2+2b^2\lambda-2b\lambda+b^2-2b+1\right)^3\right)\left)\wedge(1/3)\right)-$$
$$\left(-\frac{\left(-b-5\lambda+1\right)^3}{8\lambda^3}+\frac{\left(4\lambda^2+b\lambda-3\lambda+b-1\right)\left(-b-5\lambda+1\right)}{\lambda^3}-\right.$$
$$\left.\frac{4\left(-\lambda^2+3\lambda+2\right)}{\lambda^2}\right)/$$
$$\left(4\sqrt{\left(\frac{\left(-b-5\lambda+1\right)^2}{16\lambda^2}-\frac{4\lambda^2+b\lambda-3\lambda+b-1}{3\lambda^2}+\frac{1}{6\sqrt[3]{2}\,\lambda^2}\right.\right.$$
$$\left(\left(2\left(4\lambda^2+b\lambda-3\lambda+b-1\right)^3-144\left(-\lambda-1\right)\lambda^2\left(4\lambda^2+b\lambda-3\lambda+b-1\right)-\right.\right.$$
$$\left.\left.9\left(-5\lambda^2-b\lambda+\lambda\right)\left(-\lambda^2+3\lambda+2\right)\left(4\lambda^2+b\lambda-3\lambda+b-1\right)+27\right.\right.$$

$$
\begin{aligned}
&(-\lambda-1)\left(-5\lambda^2-b\lambda+\lambda\right)^2+54\lambda^2\left(-\lambda^2+3\lambda+2\right)^2+\\
&\sqrt{\left(\left(2\left(4\lambda^2+b\lambda-3\lambda+b-1\right)^3-144(-\lambda-1)\lambda^2\left(4\lambda^2+b\lambda-\right.\right.\right.}\\
&\qquad\left.\left.\left.3\lambda+b-1\right)-9\left(-5\lambda^2-b\lambda+\lambda\right)\left(-\lambda^2+3\lambda+2\right)\right.\right.\\
&\qquad\left.\left(4\lambda^2+b\lambda-3\lambda+b-1\right)+27(-\lambda-1)\right.\\
&\qquad\left.\left(-5\lambda^2-b\lambda+\lambda\right)^2+54\lambda^2\left(-\lambda^2+3\lambda+2\right)^2\right)^2-\\
&\qquad4\left(\lambda^4+5b\lambda^3+b^2\lambda^2+11b\lambda^2-2\lambda^2+2b^2\lambda-\right.\\
&\qquad\left.\left.2b\lambda+b^2-2b+1\right)^3\right)\Big)\,\hat{}\,(1/3)\Big)+\\
&\left(\lambda^4+5b\lambda^3+b^2\lambda^2+11b\lambda^2-2\lambda^2+2b^2\lambda-2b\lambda+b^2-2b+1\right)/\\
&\left(3\,2^{2/3}\lambda^2\left(2\left(4\lambda^2+b\lambda-3\lambda+b-1\right)^3-\right.\right.\\
&\qquad144(-\lambda-1)\lambda^2\left(4\lambda^2+b\lambda-3\lambda+b-1\right)-\\
&\qquad9\left(-5\lambda^2-b\lambda+\lambda\right)\left(-\lambda^2+3\lambda+2\right)\left(4\lambda^2+b\lambda-3\lambda+b-1\right)+\\
&\qquad27(-\lambda-1)\left(-5\lambda^2-b\lambda+\lambda\right)^2+54\lambda^2\left(-\lambda^2+3\lambda+2\right)^2+\\
&\qquad\sqrt{\left(\left(2\left(4\lambda^2+b\lambda-3\lambda+b-1\right)^3-144(-\lambda-1)\lambda^2\left(4\lambda^2+b\lambda-\right.\right.\right.}\\
&\qquad\qquad\left.\left.\left.3\lambda+b-1\right)-9\left(-5\lambda^2-b\lambda+\lambda\right)\left(-\lambda^2+3\lambda+2\right)\right.\right.\\
&\qquad\qquad\left.\left(4\lambda^2+b\lambda-3\lambda+b-1\right)+27(-\lambda-1)\right.\\
&\qquad\qquad\left.\left(-5\lambda^2-b\lambda+\lambda\right)^2+54\lambda^2\left(-\lambda^2+3\lambda+2\right)^2\right)^2-\\
&\qquad\qquad4\left(\lambda^4+5b\lambda^3+b^2\lambda^2+11b\lambda^2-2\lambda^2+\right.\\
&\qquad\qquad\left.\left.\left.\left.2b^2\lambda-2b\lambda+b^2-2b+1\right)^3\right)\Big)\,\hat{}\,(1/3)\Big)\right)\right)\right)
\end{aligned}
$$

References

[1] G. Nogues, A. Lupascu, A. Emmert, M. Brune, J.-M.Raimond, and S. Haroche, in Atom Chips, edits. J. Reichel and V. Vuletic (Wiley-VCH, Weinheim, Germany) 2011, Ch. 10, Sect. 10.3.3.

[2] N. Kryukov and E. Oks, *Can. J. Phys.*, **90**, (2012), 647.

[3] J. N. Tan, S. M. Brewer, and N. D. Guise, *Phys. Scripta* **T144**, (2011), 014009.

[4] N. Kryukov and E. Oks, *Intern. Review of Atomic and Molecular Phys.* **3**, (2012), 17.

[5] J. S. Dehesa, S. Lopez-Rosa, A. Martinez-Finkelshtein, and R. J. Janez, *Intern. J. Quantum Chemistry* **110**, (2010), 1529.

[6] T. Nandi, *J. Phys. B: At. Mol. Opt. Phys*. **42**, (2009), 125201.

[7] U. D. Jentschura, P. J. Mohr, J. N. Tan, and B. J. Wundt, *Phys. Rev. Letters* **100**, (2008), 160404.

[8] M. R. Flannery and E. Oks, *European Phys. Journal* D**47**, (2008), 27.

[9] A. V. Shytov, M. I. Katsnelson and L. S. Levitov, *Phys. Rev. Letters* **99**, (2007), 246802.

[10] M. Devoret, S. Girvin, and R. Schoelkopf, *Ann. Phys*. **16**, (2007), 767.

[11] M. R. Flannery and E. Oks, *Phys. Rev. A* **73**, (2006), 013405.

[12] E. Oks, *Stark Broadening of Hydrogen and Hydrogenlike Spectral Lines in Plasmas: The Physical Insight* (Alpha Science International, Oxford) 2006, Appendix A.

[13] E. Oks, *Eur. Phys. J*. D **28**, (2004), 171.

[14] L. Holmlid, J. Phys.: Condensed Matter **14**, (2002), 13469.

[15] S. K. Dutta, D. Feldbaum, A. Walz-Flannigan, J. R. Guest, and G. Raithel, *Phys. Rev. Lett*. **86**, (2001), 3993.

[16] E. Oks, *Phys. Rev. Letters* **85**, (2000), 2084.

[17] E. Oks, *J. Phys. B: Atom. Mol. Opt. Phys*., **33**, (2000), 3319.

[18] H. Carlsen and O. Goscinski, *Phys. Rev.* A **59**, (1999), 1063.

[19] R. P. Drake, *High-Energy-Density-Physics: Fundamentals, Inertial Fusion, and Experimental Astrophysics* (Springer, Berlin) 2006, Sect. 3.2.2.

[20] S. Atzeni and J. Meyer-ter-Vehn, *The Physics of Inertial Fusion: Beam Plasma Interaction, Hydrodynamics, Hot Dense Matter* (Oxford Univ. Press, New York) 2004, Sect. 10.1.4.

[21] D. Salzmann, *Atomic Physics in Hot Plasmas* (Oxford University Press, Oxford) 1998, Chapters 2, 22. M.S. Murillo and J.C. Weisheit, Phys. Rep., **302**, (1998), 1.

[23] H. R. Griem, *Principles of Plasma Spectroscopy* (Cambridge University Press, Cambridge) 1997, Sects.5.5, 7.3.

[24] J. Stein, I.B. Goldberg, D. Shalitin, and D. Salzmann, *Phys. Rev. A*, **39**, (1989), 2078.

[25] D. Salzmann, J. Stein, I. B. Goldberg, and R. H. Pratt, *Phys. Rev. A*, **44**, (1991), 1270.

[26] J. Stein and D. Salzmann, *Phys. Rev. A*, **45**, (1992), 3943.

[27] P. Malnoult, B. D'Etat, and H. Nguen, *Phys. Rev. A*, **40**, (1989), 1983.

[28] Y. Furutani, K. Ohashi, M. Shimizu, and A. Fukuyama, *J. Phys. Soc. Japan*, **62**, (1993), 3413.

[29] P. Sauvan, E. Leboucher-Dalimier, P. Angelo, H. Derfoul,T. Ceccotti, A. Poquerusse, A. Calisti, and B. Talin, *J. Quant. Spectr. Rad. Transfer*, **65**, (2000), 511.

[30] E. Oks, *Phys. Rev. E*, **63**, (2001), 057401.